

# In-Situ Synthesis of Cadmium Selenide Quantum Dots in Solvent-Free Polymer Template Demonstrating Stable Photoluminescence in Harsh Atmosphere

Qiao Wang,<sup>a</sup> Wenfei Shen,<sup>a</sup> Jin Liu,<sup>a</sup> Fan Gao,<sup>a</sup> Yao Wang,<sup>a</sup> Yanxin Wang,<sup>a</sup> Zhonglin Du,<sup>a</sup> Linjun Huang,<sup>a</sup> Mikhail Artemyev,<sup>b</sup> Haijiao Xie,<sup>c</sup> Jun Li,<sup>d</sup> Laurence A. Belfiore,<sup>a,d</sup> Jianguo Tang<sup>\*a</sup>

- a. Institute of Hybrid Materials, National Center of International Joint Research for Hybrid Materials Technology, National Base of International Sci. & Technology Cooperation on Hybrid Materials, Qingdao University, 308 Ningxia Road, Qingdao 266071, People's Republic of China.
- b. Research Institute for Physical Chemical Problems of the Belarusian State University, Minsk 220006, Belarus.
- c. Hangzhou Yanqu Information Technology Co., Ltd. Y2, 2nd Floor, Building 2, Xixi Legu Creative Pioneering Park, No. 712 Wen'er West Road, Xihu District, Hangzhou City Zhejiang Province, 310003, People's Republic of China.
- d. School of Materials Science and Engineering, Shanghai University of Engineering Science, Shanghai 201620, China
- e. Department of Chemical and Biological Engineering, School of Advanced Materials Discovery, and School of Biomedical Engineering, Colorado State University, Fort Collins, Colorado 80523, USA.

\*Corresponding author, e-mail: tang@qdu.edu.cn

---

## 1. Methods

### 1.1 Materials

Cadmium acetate ( $(\text{CH}_3\text{COO})_2\text{Cd}$ , 99.995%), Selenium (Se, 99.99%), Myristic acid (99.0%), methanol (99.9%), Trioctylphosphine (TOP, 90.0%), Poly (vinyl chloride) (K-value 59-55), Tetrahydrofuran (THF, 99.0%), N,N-Dimethylformamide (DMF,99.0%), Cadmium oxide ( $\text{CdO}$ ,99.5%), 1-Octadecene (1-ODE, 90%), Oleic acid (OA, 96%), were purchased from Aladdin. All chemicals were used as received.

### 1.2 Synthesis

#### 1.2.1 Preparation of $\text{Cd}(\text{myristate})_2$

Following a previously reported method with slight variations.<sup>1</sup> 2 mmol of cadmium acetate were dissolved in 5 mL of methanol, and 1.028 g of myristic acid in 30 mL of methanol. These two solutions were mixed through continuous stirring and the resulting white precipitate of  $\text{Cd}(\text{myristate})_2$  was collected through filtration. washed with methanol for 5 times, and vacuum-dried at 40 °C overnight.

#### 1.2.2 Preparation of TOPSe at 1 M

In a glovebox, 395 mg (0.05 mol) of Se powder was dissolved by agitation of 5 mL of TOP in a flask.

#### 1.2.3 Syntheses of QDiP-PVC

0.034 g of  $\text{Cd}(\text{myristate})_2$  (0.06 mM) and 2 mL THF were mixed in a glass bottle and stirred at 90 °C to obtain a transparent solution. Then, 0.3 g of PVC was introduced with rigorous

---

stirring to form a homogeneous blend. 60  $\mu\text{L}$  of 1 M TOPSe was added to the mixture at room temperature with stirring. After 30 mins, the transparent precursor-PVC solution was achieved. Then 300 mL of the precursor-PVC solution was spin coated on  $1.5 \times 1.5 \times 0.5 \text{ cm}^3$  glass sheet at 3500 rpm for 40s. After evaporation of the solvent, the precursors-PVC composite (PPC-PVC) was obtained. PPC on glass substrate was thermally treated at 160  $^\circ\text{C}$  for different time. After cooling down to a room temperature, the samples of CdSe QDs in PVC (QDiP-PVC) were obtained for further characterizations.

#### **1.2.4 Synthesis of QDiP-PVDF**

0.034 g of Cd(myristate)<sub>2</sub> and 3 ml a blended solvent (v(THF): v(DMF)=1:1) were mixed in a glass bottle and stirred at 90  $^\circ\text{C}$  to obtain a transparent solution. Then, 0.2 g of PVDF was introduced with rigorous stirring to form a homogeneous blend. Further, 60  $\mu\text{L}$  of 1 M TOPSe was added into the mixture at room temperature with stirring. After 30 min, the transparent precursors-PVDF solution was achieved. Then 300 mL of the solution was spin-coated on a  $1.5 \times 1.5 \times 0.5 \text{ cm}^3$  glass sheet at 3500 rpm for 40s. After solvent evaporation, the PPC-PVDF film was obtained. The film loading upon on glass substrate was thermal treated on a heat plate at 190  $^\circ\text{C}$  for different time. After cooling down to a room temperature, QDiP-PVDF composite was obtained

#### **1.2.5 Preparations of reference samples**

Pristine green-emitting CdSe QDs as a reference sample with PL  $\lambda_{\text{max}} = 525 \text{ nm}$  were synthesized following the reported method with slight modification.<sup>2</sup> The physical blend of CdSe QDs with the polymer film (QDbP) was prepared by mixing as-synthesized green-

---

emitting CdSe QDs and PVC in THF to a transparent solution and then spin-coated on a glass with 3500 rpm for 40 s. After solvent evaporation, the QDbP-PVC was obtained. It is worth to mention that prepared QDbP-PVC and QDiP-PVC samples contained the same amount of precursors.

### **1.3 Thermal and moisture stability tests**

QDiP-PVC, QDiP-PVDF and pristine CdSe QDs and QDbP-PVC were exposed in saturated water vapor at 40, 60, 70, 80, and 100 °C respectively. The PL intensities were tested after 24 h of exposure. The CdSe-QDiP was exposed in 60 °C saturated vapor for 30 days and PL intensities were monitored periodically. To test the stability of withstanding water, the three samples were immersed into water for 24 h. To test the stability of samples against aggressive media, QDiP-PVC, QDiP-PVDF, pristine CdSe QDs and QDbP-PVC were submerged into 0.5 M H<sub>2</sub>SO<sub>4</sub>, 0.5 M NaOH solutions and ethanol for 7 days. The PL intensities corresponding to the samples prepared above were recorded at the beginning and after 24 h.

### **1.4 Fabrication of GaN chip device with QDiP-PVC film**

Precursors-PVC solution was spin-coated on the GaN chip device plate and evaporating the solvent totally at 25 °C for 2 h. The device with PPC-PPC film was placed in an oven for thermal treatment at 160 °C for 120s in air. The GaN chip device with QDiP film was the connected to the external driving circuit for Electroluminescence measurement.

### **1.5 Inkjet printing**

The precursors of CdSe QDs and PVC were dissolved in a mixed solvent of THF and DMF (2:3 in volume) to form the precursor ink. Inkjet printing was performed using a piezoelectric

---

inkjet printer (EHDjet, Sygole). Nozzles with a diameter of 30  $\mu\text{m}$  (Dimatix) were used to eject the ink. Inkjet printing was performed using a piezoelectric inkjet printer. Nozzles with a diameter of 10  $\mu\text{m}$  (Dimatix) were used to eject the ink. Precursor inks was printed with a drop velocity of 40  $\text{mm s}^{-1}$ , drop frequency 200ms per drop and drop spacing of 100  $\mu\text{m}$  by maintaining the glass substrate at room temperature in ambient conditions. After the evaporation of solvents, place the glass substrate upper loading precursor pattern on a heat plate at 160  $^{\circ}\text{C}$  for 120 s forming the CdSe QDs patterns.

## 1.6 Characterizations

UV-vis spectra of films were measured by an ultraviolet–visible spectrometer (PerkinElmer Lambda 750S) with 2 nm at 25  $^{\circ}\text{C}$ . In this instrument, an integrated sphere was used to minimize scattering effects. PL spectra, PL life time and PLQY of films samples were realized by a fluorescence spectrophotometer (Hitachi F-4600) with a 75 W xenon lamp, using an excitation wavelength at 360 nm. The monitor wavelength for PL decay is 400~800 nm and the multi-exponential fitting model is present in below (Equation 1). PL QY were accessed using an integrating sphere apparatus. FT-IR spectra of PVC film and composites films were obtained with Nicolet 5700 Fourier transform infrared spectrometer (Thermo Fisher Scientific). The measurements were conducted in the transmission mode with resolution 4  $\text{cm}^{-1}$ . AFM topographic images were obtained using the AFM Cypher VRS model with non-contact mode to avoid the damage of film samples. Binding energies were determined by using XPS on a Thermo Scientific Escalab 250Xi. The excitation source is Al  $\text{K}\alpha$  beam (400  $\mu\text{m}$  beam spot).  $^{13}\text{C}$ -NMR spectra were measured with Bruker AVANCE III HD 400 MHz. All the

---

XPS spectra were calibrated by shifting the detected carbon C 1s peak to 284.8 eV. TEM was performed on a Tecnai G2 F20 electron microscope operating at 200 kV. Elemental maps were obtained using high-resolution STEM-EDX setup in Tecnai G2 F20 S-TWIN instrument. Slices of samples were placed on holey carbon grids for above two tests. X-ray absorption near edge structure (XANES), extended X-ray absorption fine structure (EXAFS) spectroscopy were obtained on Beamline BL14W1 synchrotron. <sup>13</sup>C-NMR spectra were measured with Bruker AVANCE III HD 400 MHz.

$$I(t)=A+B_1\exp(-t/t_1)+B_2\exp(-t/t_2) \quad \text{Equation 1}$$

### 1.7 Computational method

We have employed the Vienna Ab Initio Package (VASP)<sup>3, 4</sup> to perform all the density functional theory (DFT) calculations within the generalized gradient approximation (GGA) using the PBE<sup>5</sup> formulation. We have chosen the projected augmented wave (PAW) potentials<sup>6, 7</sup> to describe the ionic cores and take valence electrons into account using a plane wave basis set with a kinetic energy cutoff of 400 eV. Partial occupancies of the Kohn–Sham orbitals were allowed using the Gaussian smearing method and a width of 0.05 eV. The electronic energy was considered self-consistent when the energy change was smaller than 10<sup>−5</sup> eV. A geometry optimization was considered convergent when the force change was smaller than 0.02 eV/Å. Grimme’s DFT-D3 methodology<sup>8</sup> was used to describe the dispersion interactions.

The Cd<sub>41</sub>Se<sub>41</sub> cluster was truncated out of CdSe bulk in a cubic box with a side length of 30 Å. In another model, the surface of Cd<sub>41</sub>Se<sub>41</sub> cluster was covered by PVC and PVDF dimers and trimers in the mode that each exposed Cd atom binds to a halogen atom. During structural

optimizations, the  $\Gamma$  point in the Brillouin zone was used for k-point sampling, and all atoms were allowed to relax.

## 2. Supporting Figures and Tables

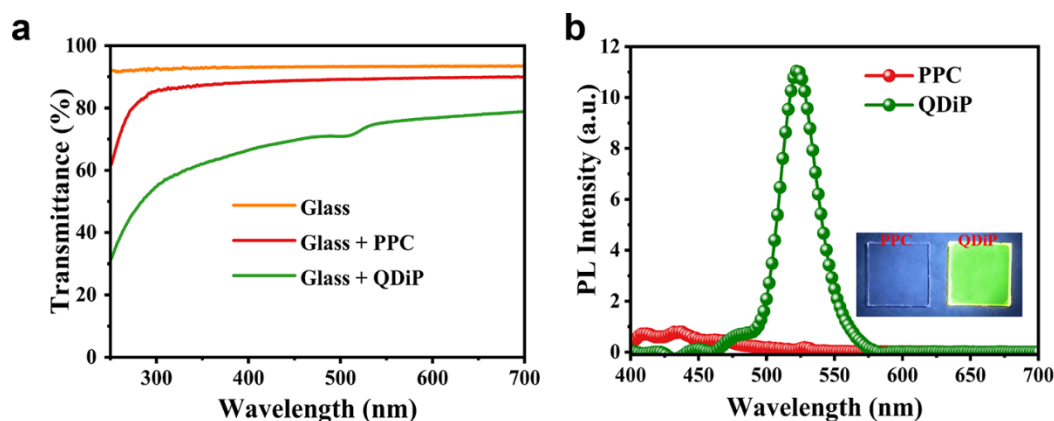
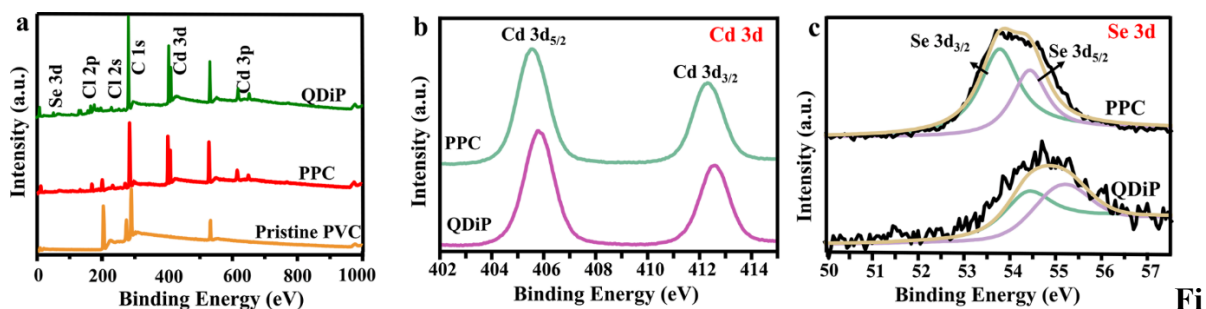


**Fig. S1.** **a** Transmittance spectra of bare glass substrate and the glass substrate coated with PPC and QDiP. **b** PL spectra of PPC-PVC and QDiP-PVC samples with  $\lambda_{\text{ex}}=360$  nm, and their images (inset) obtained under UV light ( $\lambda=365$  nm).

As shown in Fig.S1a PVC impregnated with precursors (PPC) forms a transparent film atop the glass substrate. After thermal treatment at 160 °C when precursors react with formation of CdSe QDs QDiP film demonstrates optical absorption in the blue-green range (Fig. S1a) with the broad exciton peak around  $\lambda=510$  nm. Parallel, an intense green fluorescence appears peaked at  $\lambda\approx 525$  nm (Fig. S1b)



**g. S2. a**, XPS survey spectra of pristine PVC, PPC and QDiP-PVC. Cd 3d (**b**) and Se 3d bands (**c**) of PPC-PVC and QDiP-PVC.

XPS survey spectra of pristine PVC, PPC-PVC and QDiP-PVC (Fig. S2a) show clear signals of C, Cl, O and Cd, Se for QDiP and PPC. Compared with QDiP the two peaks of Cd 3d and Se 3d bands in PPC shift to the low binding energy (Fig. S2b,c) indicating the formation of CdSe phase from the precursors in PVC.<sup>9</sup>

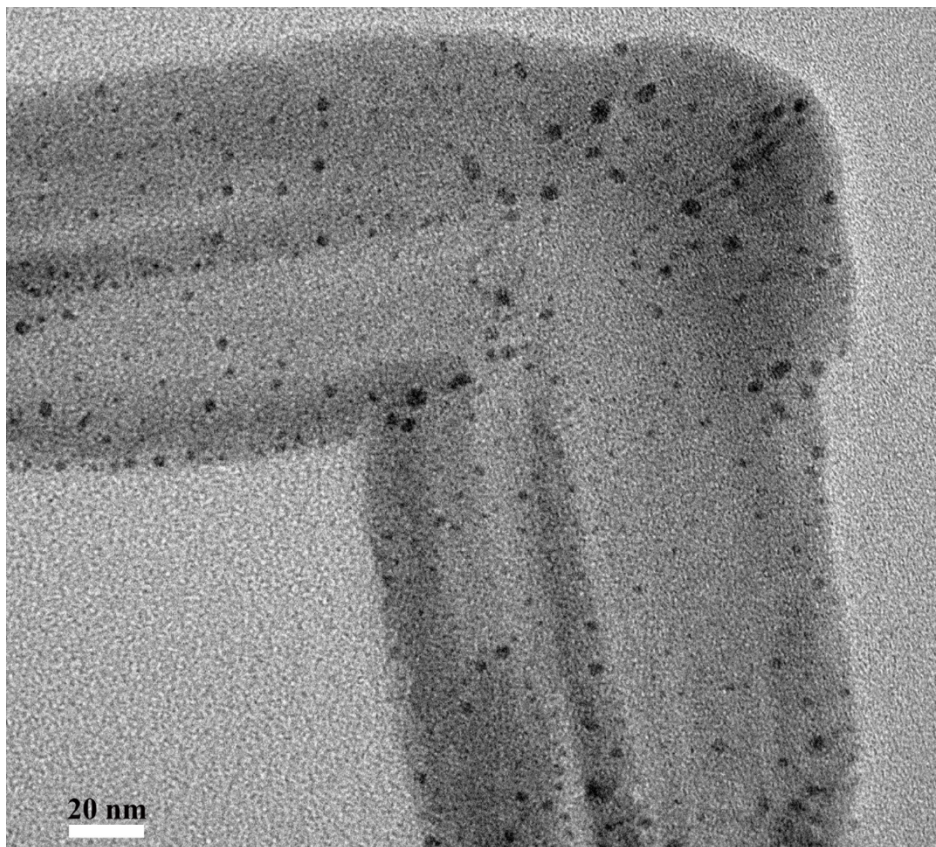


**Fig. S3.** TEM images of a complete slice of QDiP-PVC.

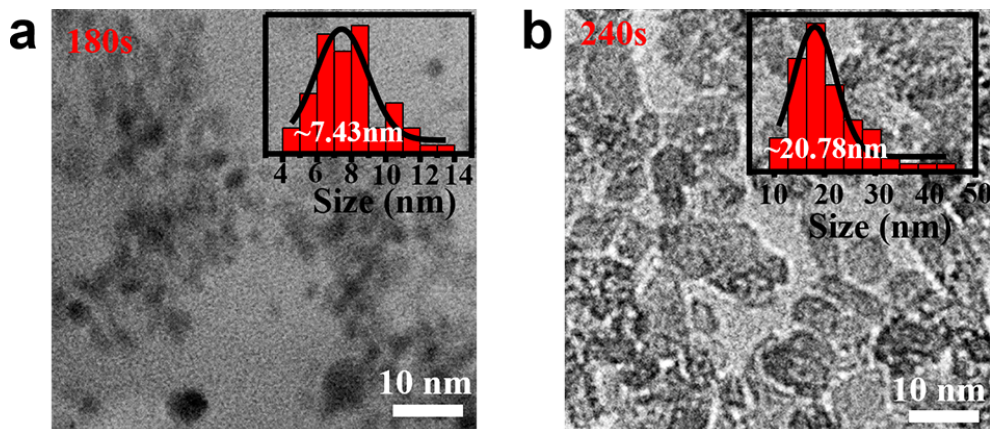


**Fig. S4.** TEM images of QDiP-PVC prepared at 160 °C for 180 s (a) and 240s (b)

While, from 120s to 180s of the reaction time the nanoparticle size increases by only 0.6 nm (from 2.97 to 3.51 nm), the growth rate is slowing down due to a decline in in-situ precursors.

At a longer reaction time the diffusion accelerates. As a result, the average size of QDs increases to ~7.43 at 180 s and ~20.78 at 240 s with a higher growth rate (Fig. S3a, b)

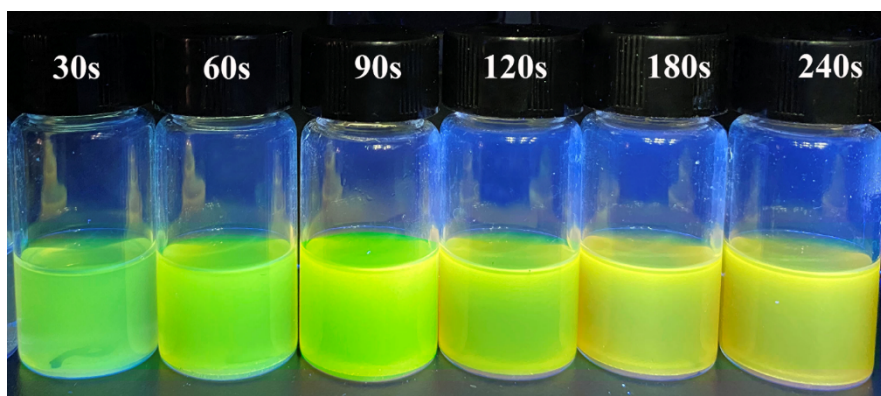


**Fig. S5. The photo of QDiP-PVC prepared with different heating time dissolved in THF under UV light (360 nm).**

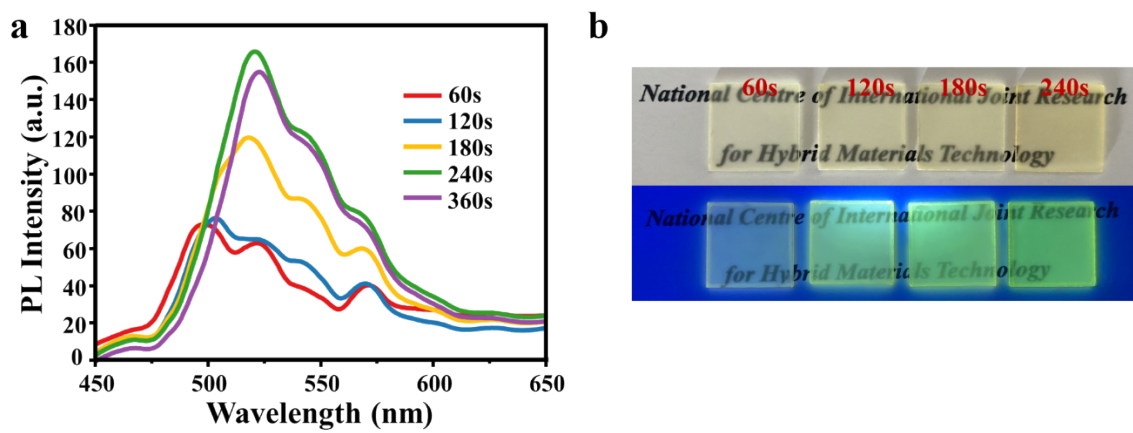


**Fig. S6.** PL spectra of QDiP-PVDF prepared at 160 °C and a different thermal treatment time and corresponding images under daylight (above) and UV light (bottom).

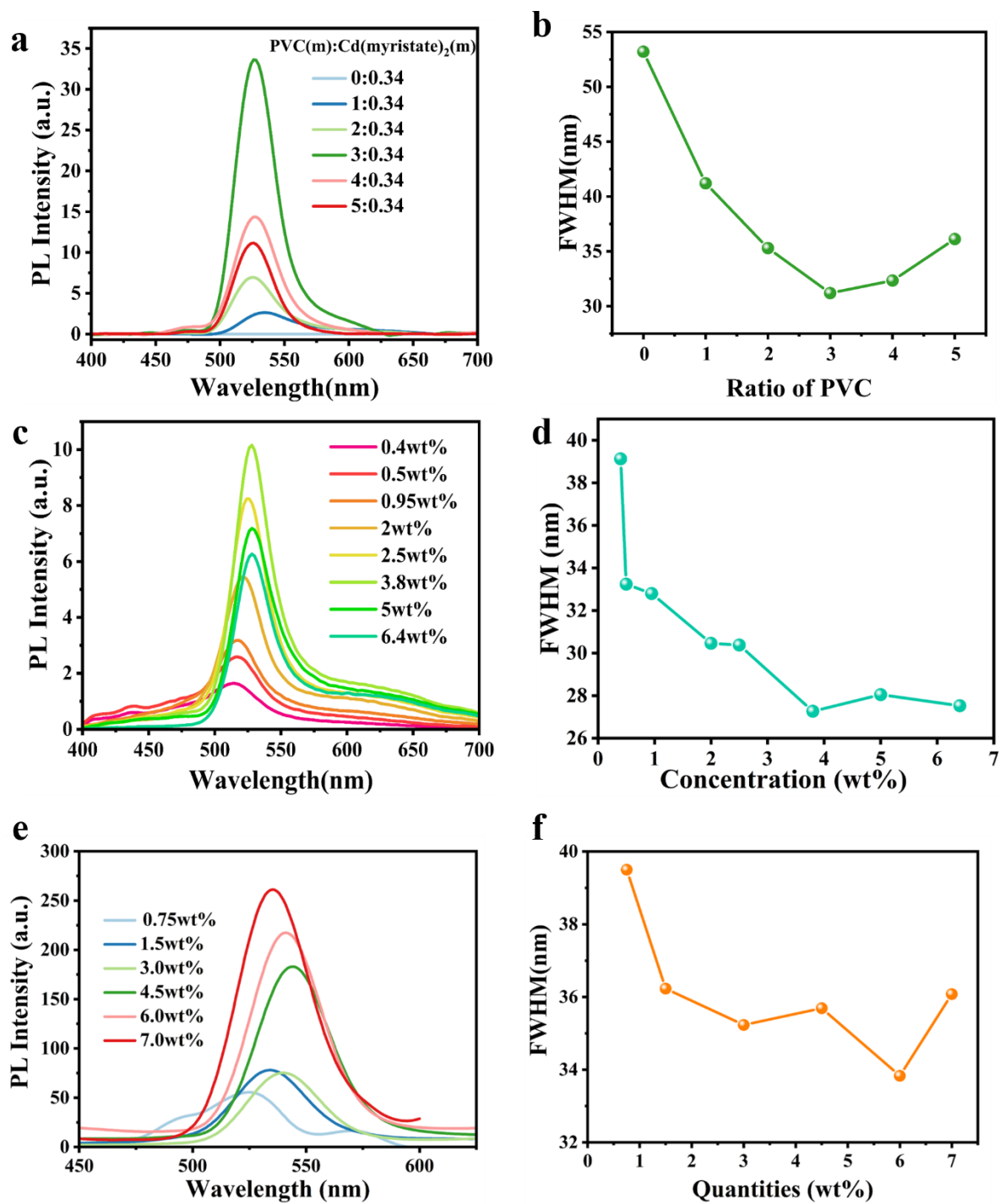


**Fig. S7.** PL spectra of QDiP-PVC (a) and corresponding FWHM (b) with increasing ratio of PVC. PL spectra of QDiP-PVC (c) and QDiP-PVDF (e),  $\lambda_{\max}$  position and FWHM of QDiP-PVC (d) and FWHM of QDiP-PVDF (f) with increasing precursor ration. QDiP-PVC were

---

prepared at 160 °C for 120 s and QDiP-PVDF at 190 °C for 60s. FWHMs were obtained from the Gaussian fitting of corresponding emission spectra.

PVC as host medium works as a template to dissolve precursors and confine the growing QDs. With the increasing of the mass ratio of PVC to Cd(myristate)<sub>2</sub>, the PL intensity reaches maximum and then decreases (Fig. S5a) and the FWHM follows the same trend. (Fig. S5b). The role of PVC to confine QDs becomes stronger with increasing PVC content in the hybrid material. However, when the PVC to Cd(myristate)<sub>2</sub> ratio surpasses 3:0.34 the precursor diffusion slows down blocking the growth of QDs. In Fig. S5c, with the increase of the total Cd/Se concentration(n(Cd): n(Se)=1:1) from 0.4 to 6.4 wt.% the strongest PL signal appears at 3.8 wt.%. Within the studied precursor concentration range the PL peak position gradually shifts from  $\lambda=513$  nm to 528 nm with FWHM decreasing from 39 nm to 27 nm as shown in Fig. S5d. The optimum 3.8 wt.% precursors concentration demonstrates the PVC template effect, i.e., the balance between the precursor diffusion and a growth confinement of QDs. Based on the obtained results we chose QDiP prepared at 160 °C, 120 s with 0.3 g PVC and 3.8 w.t% precursors as the sample for further investigation. Whithin the PVDF as the host medium the maximum of PL signal rises with the the Cd/Se concentration. While, the FWHMs show a tendency to decrease from 0.75 wt% to 6.0 wt% (Fig. S5e), and then increase when the concentration reaches 7.0 wt% (Fig. S5f). Comparing to PVC, PVDF could allow more Cd and Se atoms to be involved into the reaction, probably due to a more polar domain character in PVDF.

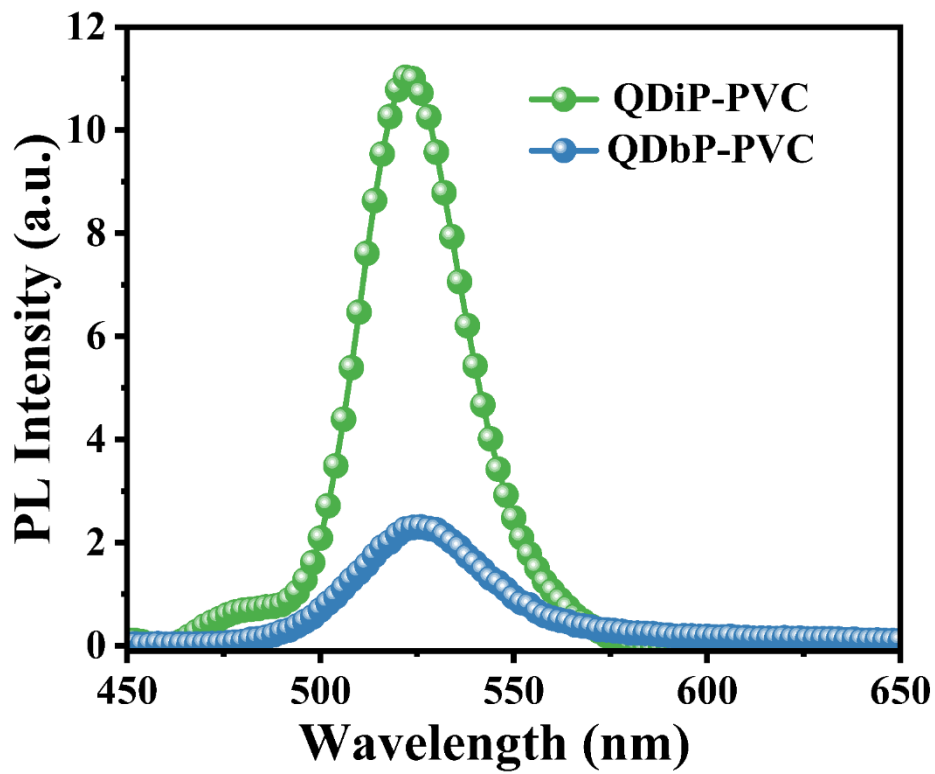


**Fig. S8.** PL spectra of QDiP-PVC and QDbP-PVC samples ( $\lambda_{\text{ex}}=360\text{nm}$ ).

**Fig. S8.** shows that CdSe-QDiP demonstrates a stronger PL signal than CdSe-QDbP when they contain the equivalent amounts of Cd and Se, which demonstrates the superiority of in situ method as compared to a physical mixing.

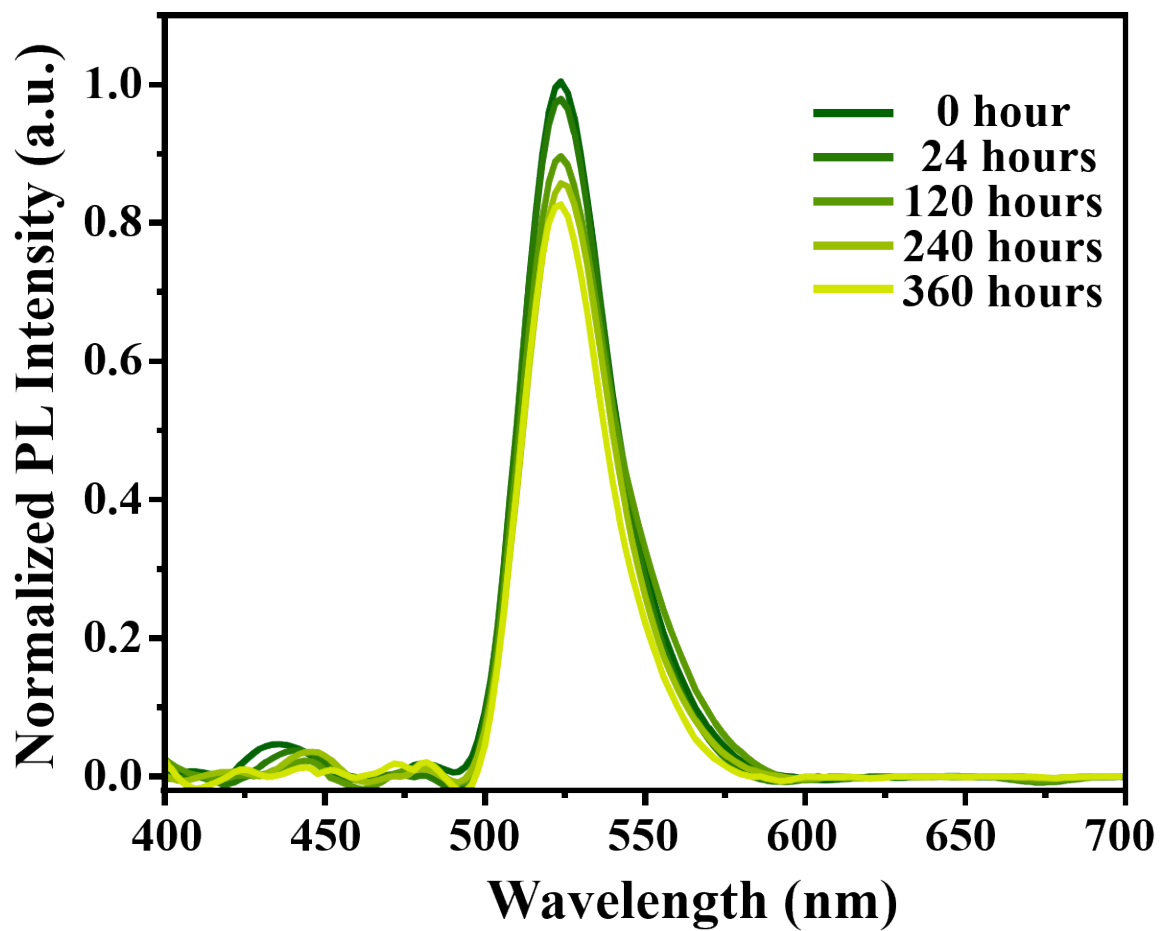


**Fig. S9.** Normalized PL intensities of QDiP-PVC sample versus treatment time in simulated sunlight at room temperature.

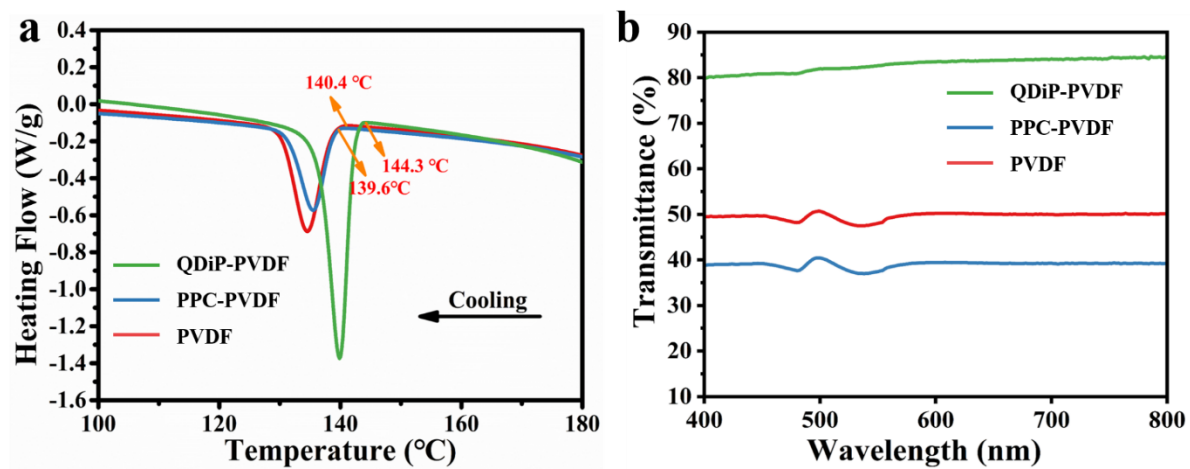
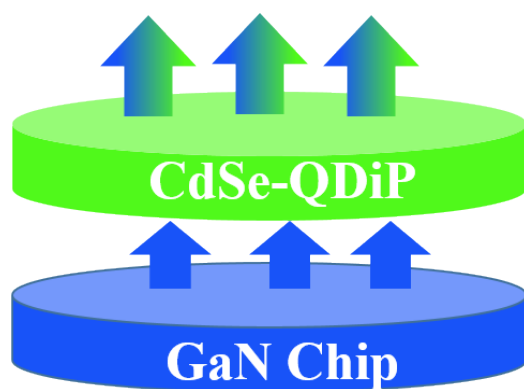


**Fig. S10.** DSC spectra (a) and optical transmittance spectra (b) of PVDF, PPC-PVDF and QDiP-PVDF.

---

**Blue and Green Light**



**Blue backlight emit**

**Fig. S11.** The scheme of the as-fabricated LED device composed of a GaN blue chip and CdSe-QDiP film.

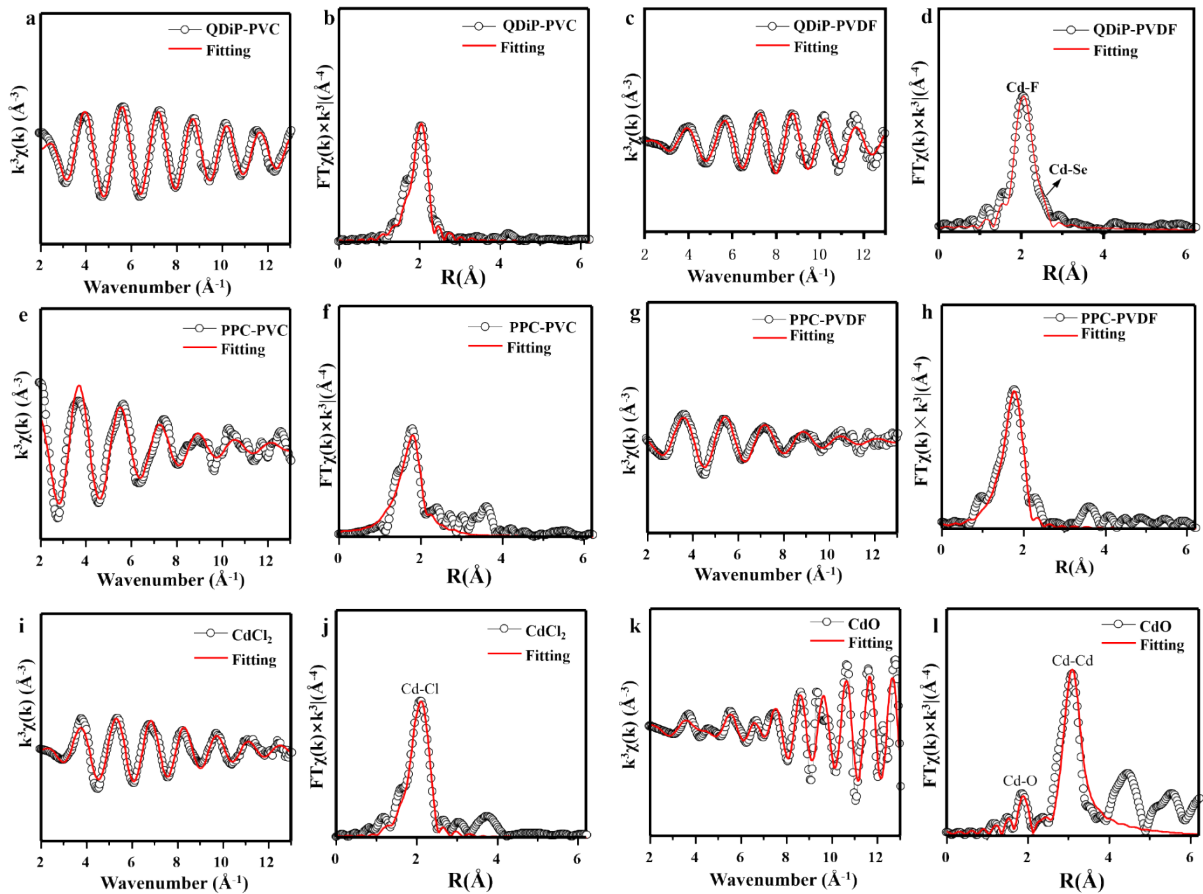


**Fig. S12.** Corresponding EXAFS fitting curves for QDiP, PPC, bulk CdCl<sub>2</sub> and CdO: **(a, c, e, g, i, k)** at k space and **(b, d, f, h, j, l)** at R space.

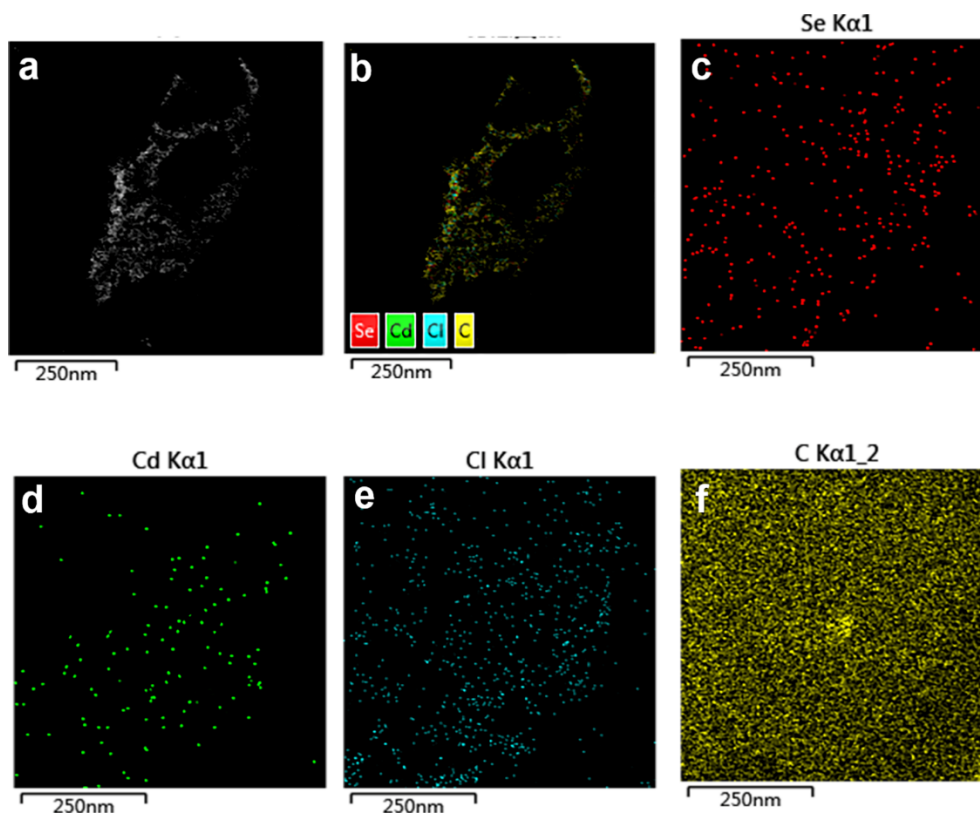


**Fig. S13 a**, STEM- HAADF image of QDiP-PVC. STEM-EDX elemental maps for sum of elements **(b)** and separated Se, Cd, Cl and C elements of QDiP-PVC **(c-f)**.

The spatial distributions of Cd, Se, Cl and C species in QDs in QDiP were revealed by the high angle annular dark field STEM (HAADF-STEM) (Fig. S10) and corresponding elemental mapping. The results show that Cd and Se mostly locate in the area of QD sites, most Cl is distributed uniformly in where s distributed uniformly in where Cd and Se are locating. The interaction between PVC matrix with CdSe QDs surface were analyzed also by solid  $^{13}\text{C}$ NMR and FT-IR spectroscopies. Fig. S11a shows that the  $^{13}\text{C}$ NMR peaks for carbons of precursor appear in PPC-PVC and QDiP-PVC, but do not appear in PVC. Comparing with PPC, QDiP-PVC shows 4 ppm deviation in the chemical shift of peak 2 for the carbons adjacent to C-Cl in

---

QDiP-PVC. That means that the coordination of Cl atoms with CdSe QDs affects the electron spin resonance of neighbor carbons of C-Cl in PVC. FTIR spectra illustrate that the presence of CdSe QDs in QDiP results in the increase of -CH<sub>2</sub>- vibration bands at 2920 and 2862 cm<sup>-1</sup> stronger, while C-Cl stretching vibration ( $\nu_{\text{C-Cl}}$ ) in QDiP at 700-600 cm<sup>-1</sup> becomes slightly weaker.<sup>10</sup>(Fig. S11b)

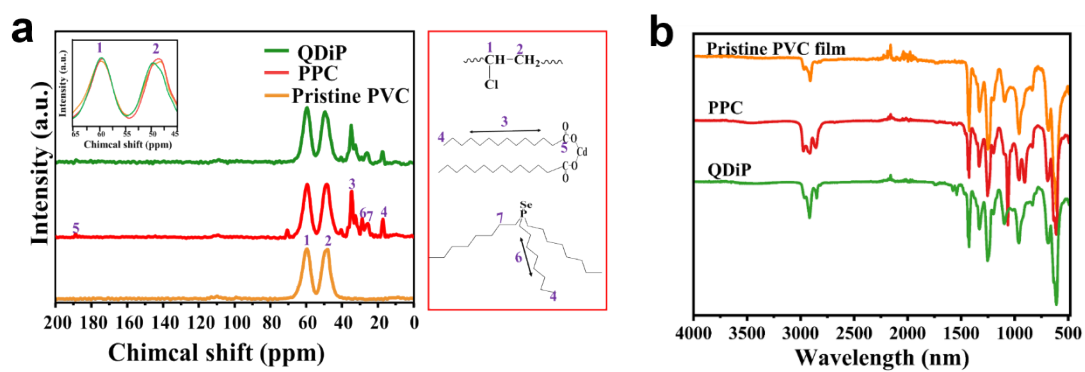


**Fig. S14**  $C^{13}$ -NMR (**a**) and FTIR (**b**) spectra of pristine PVC, PPC-PVC and QDiP-PVC samples.

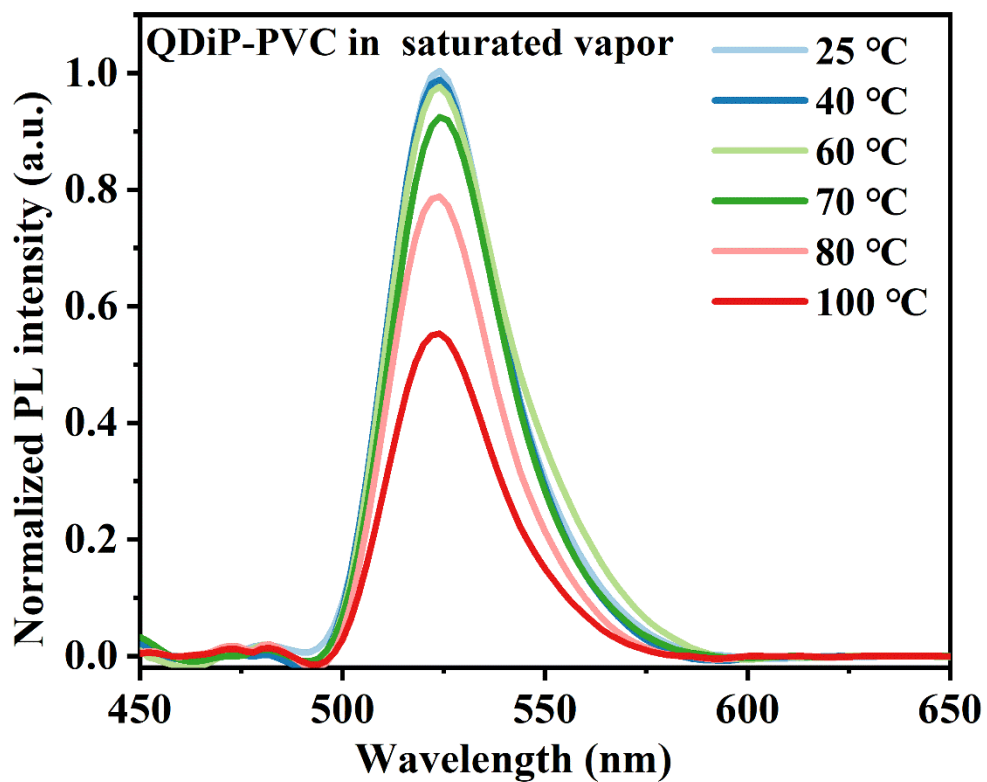


**Fig. S15** The PL spectra of QDiP-PVC after 24 hours in saturated vapor at different temperatures.

---

**Fig. S14**  $C^{13}$ -NMR (a) and FTIR (b) spectra of pristine PVC, PPC-PVC and QDiP-PVC samples.

**Table S1.** EXAFS fitting parameters at the Cd K-edge for various samples

Sample	Shell	CNa	$\sigma^2(\text{\AA}^2)$ c	R factor
CdO	Cd-O	6*	0.0044	0.0125
	Cd-Cd	12*	0.0015	
CdCl <sub>2</sub>	Cd-Cl	6.0±0.3	0.0092	0.0139
PPC-PVC	Cd-O	4.6±0.8	0.0063	0.0141
QDiP-PVC	Cd-Se/Cl	2.6±0.4	0.0022	0.0184
PPC-PVDF	Cd-O/F	5.6±0.3	0.0103	0.0139
QDiP-PVDF	Cd-F	2.5±0.6	0.0036	0.0196
	Cd-Se	0.8±0.4	0.0067	

---

---

## Reference

1. S. Ithurria, G. Bousquet and B. Dubertret, *Journal of the American Chemical Society*, 2011, **133**, 3070-3077.
2. C. Y. Zhu, Q. Wang, G. R. Sun, S. Zhao, Y. Wang, T. H. Li, X. L. Hao, M. Artemyev and J. G. Tang, *Nanomaterials*, 2022, **12**.
3. G. Kresse and J. Furthmuller, *Computational Materials Science*, 1996, **6**, 15-50.
4. G. Kresse and J. Furthmuller, *Physical Review B*, 1996, **54**, 11169-11186.
5. J. P. Perdew, K. Burke and M. Ernzerhof, *Physical review letters*, 1996, **77**, 3865-3868.
6. G. Kresse and D. Joubert, *Physical Review B*, 1999, **59**, 1758-1775.
7. P. E. Blochl, C. J. Forst and J. Schimpl, *Bulletin of Materials Science*, 2003, **26**, 33-41.
8. S. Grimme, J. Antony, S. Ehrlich and H. Krieg, *Journal of Chemical Physics*, 2010, **132**.
9. S. N. Sharma, H. Sharma, G. Singh and S. M. Shivaprasad, *Nuclear Instruments and Methods in Physics Research Section B: Beam Interactions with Materials and Atoms*, 2006, **244**, 86-90.
10. J. V. Antony, P. Kurian, N. P. N. Vadakkedathu and G. E. Kochimoolayil, *Industrial & Engineering Chemistry Research*, 2014, **53**, 2261-2269.